Quantum-nondemolition criteria in traveling-wave second-harmonic generation

M. K. Olsen,[1,2] L. I. Plimak,[2,3] M. J. Collett,[2] and D. F. Walls[2]
[1]*Departamento de Física Experimental, Instituto de Física, Universidade de São Paulo – USP, Caixa Postal 66318, São Paulo, SP 05389-970, Brazil*
[2]*Department of Physics, University of Auckland, Private Bag 92019, Auckland, New Zealand*
[3]*Department of Chemical Physics, The Weizmann Institute of Science, 76100 Rechovot, Israel*

(Received 19 November 1999; revised manuscript received 4 April 2000; published 13 July 2000)

Using the full nonlinear equations of motion, we calculate the quantum-nondemolition (QND) correlations for the traveling-wave second-harmonic generation. We find that, after a short interaction length, these are qualitatively different from results calculated previously using a linearized fluctuation analysis. We demonstrate that, although individual QND criteria can be very good in certain regions, there is no region where all three of the standard criteria are perfect, as has previously been claimed. We also show that only the amplitude quadrature of the output field can be considered as a QND quantity, with the phase quadrature not satisfying all the criteria.

PACS number(s): 42.50.Dv, 42.50.Lc, 42.65.−k, 42.65.Ky

I. INTRODUCTION

Traveling-wave second-harmonic generation is one of the simplest nonlinear optical processes. The classical solutions for the generated fields are well-known [1] and have been used as the basis of a linearized fluctuation analysis to calculate both the amount of squeezing present in, and the quantum-nondemolition (QND) correlations of the output fields [2–4]. However, a full nonlinear treatment of the problem, which must be done numerically, shows that even the classical solutions for the mean values of the fields are not accurate for arbitrary interaction length, with quantum noise playing a significant role in the dynamics [5,6]. Intracavity second-harmonic generation has previously been proposed as a candidate for a QND scheme [7], although most proposals utilizing $\chi^{(2)}$ media are concerned with the twin beam properties of parametric down-conversion [8].

Quantum-nondemolition measurements were originally proposed as a means of either obtaining information from a signal without degradation of the same signal, or of preparing a system in a known quantum state [9–14]. A problem with any standard measurement is that the measured quantity is perturbed, changing the quantity in an undetermined way by the addition of a *back-action* noise. The basic idea of a QND measurement is that this noise is added to a complementary observable, while the act of measurement prepares the system in a known quantum state, so that the presence of any perturbation can be detected by a subsequent measurement. Three criteria have been developed that can be used to establish the worth of any device as a QND measurement scheme [15], along with slightly different criteria that are more closely related to experiment [16,17]. Unfortunately, two of the latter criteria are only calculable in a linearized analysis, which has previously been shown to have limited validity for the present scheme. A general review of quantum-optical QND experiments along with an analysis of results using the linearized criteria shows that both $\chi^{(2)}$ and $\chi^{(3)}$ processes, as well as the interaction of light with cold atoms, can be used as QND systems [8]. Of these possibilities, the interaction of light with cold rubidium atoms in a magneto-optical trap has given the best results [18].

II. THEORETICAL MODEL

Second-harmonic generation is an optical process using a nonlinear $\chi^{(2)}$ crystal, in which a pump field at frequency ω produces a harmonic field at frequency 2ω. We consider here only the case of perfect phase matching between the two fields, with both fields considered as plane waves. In the traveling-wave regime, we can write an interaction Hamiltonian as

$$\mathcal{H}=\frac{i\hbar\kappa}{2}[\hat{a}^{\dagger\,2}\hat{b}-\hat{a}^2\hat{b}^{\dagger}], \tag{1}$$

where $\hat{a}$ and $\hat{b}$ are the annihilation operators for photons at frequencies ω and 2ω, respectively, at position z inside the nonlinear crystal, and κ represents the effective strength of the nonlinear interaction between the two modes. The operator equations for the system are found as

$$\begin{aligned}\frac{d\hat{a}}{dz}&=\kappa\hat{a}^{\dagger}\hat{b},\\ \frac{d\hat{b}}{dz}&=-\frac{\kappa}{2}\hat{a}^2,\end{aligned} \tag{2}$$

for which no analytical solution is known.

Earlier analyses of the quantum properties of the generated fields in pure second-harmonic generation have relied on an either an iteration to second order in the interaction length [19], or linearization about the classical solutions [2–4], which are found by treating the operators in Eq. 2 as c numbers. The first of these methods is only acceptable as long as z remains very small, while the second depends on the fluctuations being small compared to the expectation values of the operators. As the fluctuations in the phase quadratures are predicted to increase very rapidly, while the fundamental field is predicted to decrease monotonically, linearization is also of limited validity. In a previous analysis [5], we have shown that the classical solutions for the mean fields depart dramatically from the numerical quantum solutions at the point where the quantum noise begins to increase, graphically demonstrating the limitations to a linearized analysis of this system.

It is therefore also of interest to investigate the full nonlinear system with regard to the QND measurement criteria of Holland *et al.* [15], which must also be done numerically. There are two possibilities for performing the numerical computations: either the positive-*P* [20] or the Wigner representation [21,22]. These representations are commonly used in quantum optical problems to represent operator-valued quantities in terms of *c* numbers. Our present system can be mapped exactly onto positive-*P* equations, via the master and Fokker-Planck equations

$$\frac{d\alpha}{dz}=\kappa\alpha^{\dagger}\beta+\sqrt{\kappa\beta}\,\eta_1(z),$$

$$\frac{d\alpha^{\dagger}}{dz}=\kappa\alpha\beta^{\dagger}+\sqrt{\kappa\beta^{\dagger}}\,\eta_2(z),$$

$$\frac{d\beta}{dz}=-\frac{\kappa}{2}\alpha^2, \tag{3}$$

$$\frac{d\beta^{\dagger}}{dz}=-\frac{\kappa}{2}\alpha^{\dagger\ 2}.$$

In the above system of equations, there is a correspondence between $[\hat{a},\hat{a}^{\dagger},\hat{b},\hat{b}^{\dagger}]$ and $[\alpha,\alpha^{\dagger},\beta,\beta^{\dagger}]$, although the latter are *c*-number variables that are not complex conjugate except in the mean of a large number of stochastic trajectories. This is due to the independence of the real noise terms, which have the properties $\overline{\eta_1(z)}=\overline{\eta_2(z)}=0$ and $\overline{\eta_i(z)\,\eta_j(z')}=\delta_{ij}\delta(z-z')$.

A mapping of this system onto the Wigner representation does not result in a Fokker-Planck equation, as we find third-order terms, which can however, be dropped to result in the same system of equations as is used classically:

$$\frac{d\alpha}{dz}=\kappa\alpha^{*}\beta,$$

$$\frac{d\beta}{dz}=-\frac{\kappa}{2}\alpha^2, \tag{4}$$

with the difference that the initial conditions for each trajectory are taken from the Wigner distribution for the input states of the light fields. It has been found that for this system, the positive-*P* and truncated Wigner representations give almost identical results for the photon numbers and quadrature variances, even though the truncation signifies that some higher-order quantum effects are not included [5]. The main advantage of the Wigner representation is that it automatically calculates symmetrically ordered operator products, which are used in the definitions of the correlation functions. However, in the calculation of the correlation functions required here, the Wigner representation results are not as accurate as for photon number and quadrature variances. Therefore we have decided to present only the results of the positive-*P* simulations.

As in previous analyses of this system, we will use a scaled interaction length, $\xi=z\kappa\sqrt{Na(0)/2}$, where $Na(0)$ is the expectation value of the photon number in the fundamental entering the crystal. This allows direct comparison with analytical results obtained in a linearized analysis. For all the quantities calculated, we have assumed an input coherent state at the fundamental, with a mean value of 10^6 photons, and a vacuum at the second harmonic. We should state here that the values of $N_a(0)$ and κ used in our simulations are not particularly physical, with 10^6 being a very low photon number and 0.01 being a very high value for the effective nonlinearity. However, the important physical quantity here is $\kappa\sqrt{N_a(0)}$, used in the definition of ξ. The values used have been chosen because we have to simulate the equations on the *z* axis, and with a larger value of $N_a(0)$ and a smaller value of κ, the integration time required becomes unreasonable. A worthwhile physical comparison with our results comes from considering recent experiments that report $\approx$64% conversion efficiency [23,24]. Using the classical solution for N_a, which is valid in this region, $N_a(\xi)=N_a(0)\mathrm{sech}^2(\xi)$, we see that $\xi\approx1.1$. This means that the effects we find that differ strongly from the linearized solutions will need more effective crystals or higher-powered lasers, or both, than those that have so far been used for second-harmonic generation.

A. Correlation functions

The QND correlations calculated previously for this system [2] are those developed by Holland *et al.* [15], which refer to measurement, degradation of the signal field, and state preparation. It is worthwhile noting that other correlation functions have been defined [16,17], which are more experimentally meaningful, but are not readily applicable to a system that cannot be linearized. As it has previously been shown that the present system departs strongly from the behavior calculated in a linearized analysis, we have calculated the correlations of Holland *et al.*

Generally, in QND schemes we need a signal field and a probe field, so that measurements on the probe field can be used to derive information on the signal without perturbing the signal. The criteria used to evaluate a scheme concern the worth as a measurement device, the degradation of the signal field by measurement of the probe, and the usefulness for state preparation. These criteria are evaluated using symmetrised two-field correlation functions

$$C_{AB}^2=\frac{|\frac{1}{2}\langle AB+BA\rangle-\langle A\rangle\langle B\rangle|^2}{V(A)V(B)}, \tag{5}$$

with a value of one signifying perfect performance. In the present system, it has been proposed that both the quadratures X_a and Y_b [where $X_a=a+a^{\dagger}$ and $Y_b=-i(b-b^{\dagger})$] should satisfy the first two criteria as the correlation functions $C^2_{X_a^{out}X_a^{in}}(\xi)$, $C^2_{X_b^{out}X_a^{in}}(\xi)$, $C^2_{Y_b^{out}Y_b^{in}}(\xi)$, and $C^2_{Y_a^{out}Y_b^{in}}(\xi)$ all go to unity for large ξ in the linearized analysis.

The third criterion, on state preparation, has also been claimed to be fulfilled by X_a and Y_b, as long as Y_b can be attenuated without noise, and is characterized by the conditional variances

$$V(X_a^{out}|X_b^{out})=V[X_a(\xi)]\{1-C^2_{X_a^{out}X_b^{out}}\},$$
$$V(Y_b^{out}|Y_a^{out})=V[Y_b(\xi)]\{1-C^2_{Y_a^{out}Y_b^{out}}\}. \tag{6}$$

Our purpose is to evaluate these correlations in the full nonlinear treatment, to discover if and where the system may still be useful as a QND device.

B. Symmetrization

The calculation of the correlation functions of output fields is relatively simple, as in, for example, $C^2_{X_a^{out}X_b^{out}}$, because all the operator products involved are independent of ordering. This is not the case with the input-output correlations. To calculate these, we have two choices. We can either use the Wigner representation at the expense of losing some information, or we can calculate average multitime commutators to allow us to normally order all operator products and use the positive-P representation.

To find the average multipoint commutators, we notice that they can be calculated using Kubo's famous relation for the linear response function [25–27]. Namely, we begin by adding an interaction with complex c-number sources to the system Hamiltonian

$$H_{eff}\to H_{eff}+\int dz[s_a^*(z)\hat{a}(z)+s_a(z)\hat{a}^\dagger(z)+s_b^*(z)\hat{b}(z)+s_b(z)\hat{b}^\dagger(z)]. \tag{7}$$

Then, for an arbitrary operator $\hat{A}(z)$ (assuming $z>0$),

$$\left.\frac{\delta\langle\hat{A}(z)\rangle}{\delta s_a(0)}\right|_0=-\frac{i}{\hbar}\langle[\hat{A}(z),\hat{a}^\dagger(0)]\rangle,$$
$$\left.\frac{\delta\langle\hat{A}(z)\rangle}{\delta s_a^*(0)}\right|_0=-\frac{i}{\hbar}\langle[\hat{A}(z),\hat{a}(0)]\rangle,$$
$$\left.\frac{\delta\langle\hat{A}(z)\rangle}{\delta s_b(0)}\right|_0=-\frac{i}{\hbar}\langle[\hat{A}(z),\hat{b}^\dagger(0)]\rangle, \tag{8}$$
$$\left.\frac{\delta\langle\hat{A}(z)\rangle}{\delta s_b^*(0)}\right|_0=-\frac{i}{\hbar}\langle[\hat{A}(z),\hat{b}(0)]\rangle,$$

where ''$|_0$'' indicates that all functional derivatives are taken with zero sources. Setting $\hat{A}=\hat{a},\ \hat{a}^\dagger,\ \hat{b},\ \hat{b}^\dagger$, respectively, we express all the commutators needed as the linear response functions of the system. In turn, these functions are easily calculated numerically. It is straightforward to show that under the transformation (7), Eqs. (3) become

$$\frac{d\alpha}{dz}=\kappa\alpha^\dagger\beta+\sqrt{\kappa\beta}\,\eta_1(z)-is_a(z),$$
$$\frac{d\alpha^\dagger}{dz}=\kappa\alpha\beta^\dagger+\sqrt{\kappa\beta^\dagger}\,\eta_2(z)+is_a^\dagger(z),$$
$$\frac{d\beta}{dz}=-\frac{\kappa}{2}\alpha^2-is_b(z), \tag{9}$$
$$\frac{d\beta^\dagger}{dz}=-\frac{\kappa}{2}\alpha^{\dagger\,2}+is_b^\dagger(z).$$

In the above, $s_a^\dagger=s_a^*$ and $s_b^\dagger=s_b^*$. However, when calculating the derivatives, we may assume that s_a, $s_a^\dagger$, s_b, $s_b^\dagger$ are independent quantities. Furthermore, a derivative $\delta/\delta s_a(0)$ (say) means physically the system's reaction to the delta source $s_a(z)\propto\delta(0)$. That is, the derivatives in Eq. (8) are in fact taken by the variable initial conditions, $\alpha(0)\to\alpha(0)+d\alpha(0)$, etc. Finally,

$$\langle[\hat{A}(z),\hat{a}^\dagger(0)]\rangle=\left.\frac{\partial\langle\hat{A}(z)\rangle}{\partial\alpha(0)}\right|_0, \tag{10}$$

$$\langle[\hat{A}(z),\hat{a}(0)]\rangle=-\left.\frac{\partial\langle\hat{A}(z)\rangle}{\partial\alpha^\dagger(0)}\right|_0, \tag{11}$$

$$\langle[\hat{A}(z),\hat{b}^\dagger(0)]\rangle=\left.\frac{\partial\langle\hat{A}(z)\rangle}{\partial\beta(0)}\right|_0, \tag{12}$$

$$\langle[\hat{A}(z),\hat{b}(0)]\rangle=-\left.\frac{\partial\langle\hat{A}(z)\rangle}{\partial\beta^\dagger(0)}\right|_0. \tag{13}$$

This clearly results in correct commutators at $z=0$, e.g.,

$$\langle[\hat{a}(0),\hat{a}^\dagger(0)]\rangle=\frac{\partial\alpha(0)}{\partial\alpha(0)}=1, \tag{14}$$

$$\langle[\hat{a}^\dagger(0),\hat{a}(0)]\rangle=-\frac{\partial\alpha^\dagger(0)}{\partial\alpha^\dagger(0)}=-1, \tag{15}$$

$$\langle[\hat{a}(0),\hat{a}(0)]\rangle=-\frac{\partial\alpha(0)}{\partial\alpha^\dagger(0)}=0, \tag{16}$$

etc.

By numerical experiments, we found that assuming $d\alpha(0)$, $d\alpha^\dagger(0)$, $d\beta(0)$, $d\beta^\dagger(0)$ to be independent real quantities resulted in the sampling noise being dramatically reduced compared to that for $d\alpha^\dagger(0)=d\alpha^*(0)$ and $d\beta^\dagger(0)=d\beta^*(0)$. For smaller lengths, when the sampling noise is relatively small, both ways of calculating commutators were shown to lead to identical results.

Having calculated all the commutators numerically, we write the covariances in symmetrized form, so that, for example,

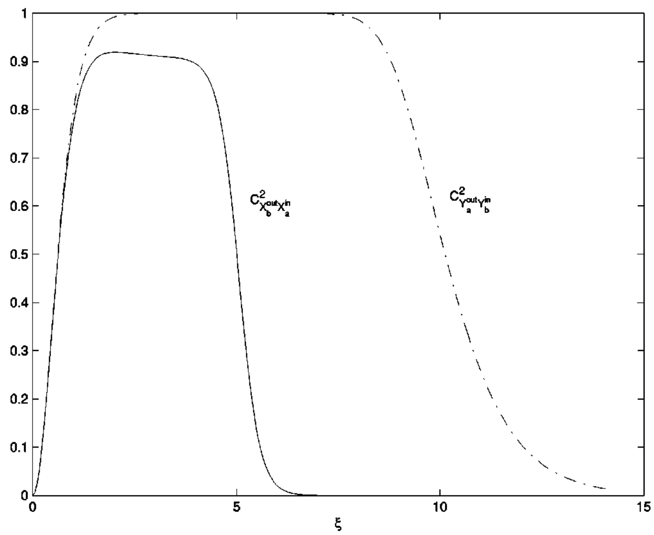

FIG. 1. The correlations $C^2_{X_b^{out}X_a^{in}}(\xi)$ and $C^2_{Y_a^{out}Y_b^{in}}(\xi)$, which quantify the worth of the scheme as a measurement device. In the linearized analysis, these two are equal and go to unity for large ξ. Note that ξ $[=z\kappa\sqrt{Na(0)/2}]$ is a dimensionless interaction length and all the values plotted are also dimensionless.

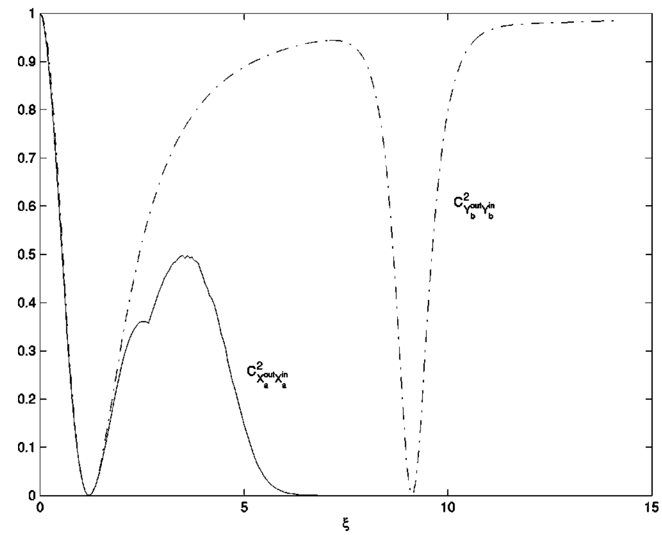

FIG. 2. The correlations $C^2_{X_a^{out}X_a^{in}}(\xi)$ and $C^2_{Y_b^{out}Y_b^{in}}(\xi)$, which quantify the degradation of the signal field. In the linearized analysis, these two are also equal and go to unity for large ξ.

$$\begin{aligned}\langle X_b^{out},X_a^{in}\rangle_{\mathrm{symm}}=&\langle b(\xi)a(0)+a^\dagger(0)b(\xi)+a^\dagger(0)b^\dagger(\xi)\\&+b^\dagger(\xi)a(0)\rangle+\frac{1}{2}\langle[b(\xi),a^\dagger(0)]\\&+[b^\dagger(\xi),a^\dagger(0)]-[b(\xi),a(0)]\\&-[b^\dagger(\xi),a(0)]\rangle-\langle X_b^{out}\rangle\langle X_a^{in}\rangle,\end{aligned}\tag{17}$$

and similarly for the other covariances.

III. RESULTS

The correlation functions have all been calculated using between 5×10^5 and 10^8 stochastic trajectories, depending on what was necessary to achieve good convergence. We used an iterative Euler algorithm, calculating the trajectories using Itô calculus, which in this case proved to be more stable than Stratonovich [28]. As expected, we find that the correlations are not as good in the full nonlinear treatment, which predicts that all are perfect for large enough ξ, but we also find other interesting behavior.

Beginning with meaurement quality, we wish to see how much information can be obtained about the input signal from a measurement of the probe output. It has been proposed that X_b^{out} and Y_a^{out} can be used as probes to give information on X_a^{in} and Y_b^{in}, respectively. In the linearized analysis, the correlations between these quantities are found to be equal and perfect for large ξ. However, we can see in Fig. 1 that $C^2_{X_b^{out}X_a^{in}}(\xi)$ and $C^2_{Y_a^{out}Y_b^{in}}(\xi)$ are no longer found to be equal after an initial short interaction length, but that $C^2_{Y_a^{out}Y_b^{in}}(\xi)$ is still almost perfect over a finite range. The utility of this for QND measurement is somewhat dubious, however, as we already know the input of mode b is a vacuum state in pure second-harmonic generation. The correlation between X_b^{out} and X_a^{in} is nearly 90% over a small length, but then rapidly vanishes as the quantum noise in the X_a quadrature rapidly increases, as shown below in Fig. 6. This is at the same point that $N_a(\xi)$ begins to revive, as seen below in Fig. 5.

The second criterion, that of signal degradation, quantifies the ability of the scheme to isolate quantum noise induced by the measurement scheme from the observable of interest, and is illustrated by $C^2_{X_a^{out}X_a^{in}}(\xi)$ and $C^2_{Y_b^{out}Y_b^{in}}(\xi)$ in Fig. 2. We see again that the correlations are not equal for the phase and amplitude quadratures, with the phase quadrature correlation becoming almost perfect for $\xi\approx7$, although this is again not particularly interesting. The reason for the sharp valley in $C^2_{Y_b^{out}Y_b^{in}}(\xi)$ around $\xi=9$ is that these two quadratures become anti-correlated at this point, as N_b reaches a local minimum and starts to increase again. It is possible that, at this point, there may be two quadratures exhibiting better correlations, with the anticorrelation being due to a quadrature rotation effect.

The output-output correlation functions $C^2_{X_a^{out}X_b^{out}}(\xi)$ and $C^2_{Y_a^{out}Y_b^{out}}(\xi)$, used to calculate the conditional variances that quantify the third criterion of state preparation, are shown in Fig. 3. These are again different and the correlation for the amplitude quadratures, by vanishing at $\xi\approx5$, shows that the X_a and X_b quadratures actually become anticorrelated after this point. Before this point, $\langle X_a\rangle$ is positive and decreasing, while $\langle X_b\rangle$ is negative and decreasing. After this point, $\langle X_a\rangle$ continues to decrease while $\langle X_b\rangle$ starts to increase, eventually becoming positive. The fact that $N_a(\xi)$ experiences a revival while $\langle X_a\rangle$ continues to decrease is because the conjugate quadrature $\langle Y_a\rangle$ has grown, something again not predicted by the linearized analysis. The conditional variances themselves are shown in Fig. 4, from which we can see that

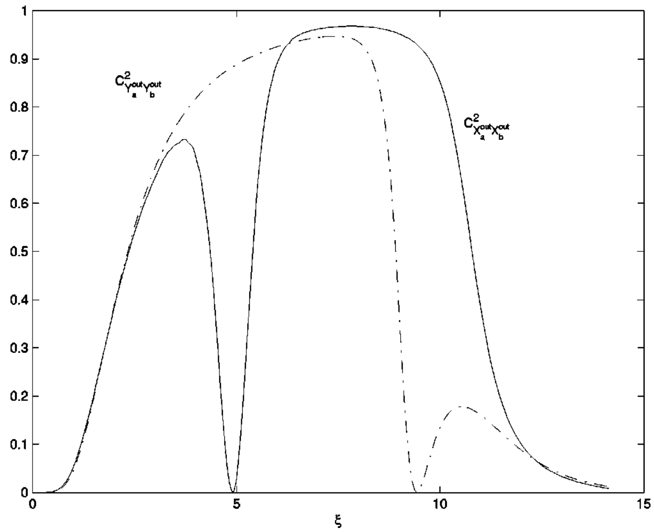

FIG. 3. The correlations $C^2_{X_a^{out}X_b^{out}}(\xi)$ and $C^2_{Y_a^{out}Y_b^{out}}(\xi)$, used to calculate the conditional variances that quantify state preparation. In the linearized analysis, these two are also equal and go to unity for large ξ.

the phase quadrature never satisfies the requirement for state preparation, while the amplitude quadrature satisfies it very well over a reasonable range of interaction length. It is however, instructive to examine the definition of the conditional variances given in Eq. (6). It is normally assumed that the conditional variance can go to zero when the appropriate correlation goes to one [15]. However, in this case $V(X_a^{out}|X_b^{out})$ is very small even in the region where $C^2_{X_a^{out}X_b^{out}}$ vanishes, due to $V(X_a)$ being very small in this region. Hence, we do not obtain good state preparation because of a strong correlation, but because the signal output is very highly squeezed. On the other hand, we find a reasonable correlation for the Y quadratures, but a large covariance due to large excess noise, so that Y_a does not satisfy the criterion for state preparation.

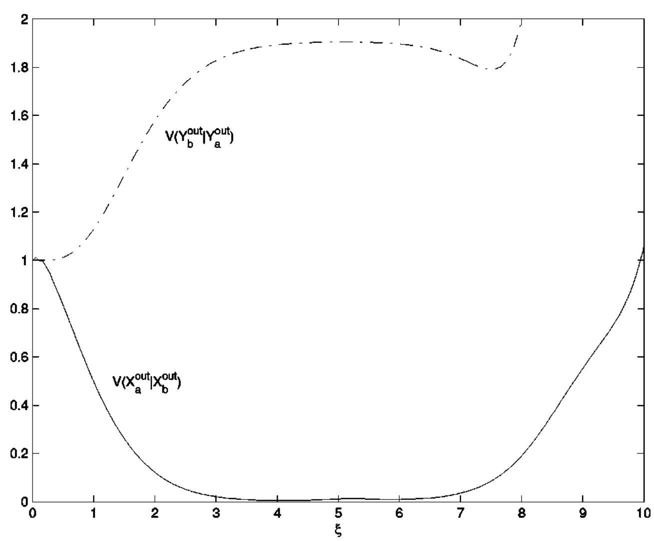

FIG. 4. The conditional variances $V(X_a^{out}|X_b^{out})$ and $V(Y_b^{out}|Y_a^{out})$, which quantify state preparation. In the linearized analysis, the first of these goes to zero and the second goes to two for large ξ.

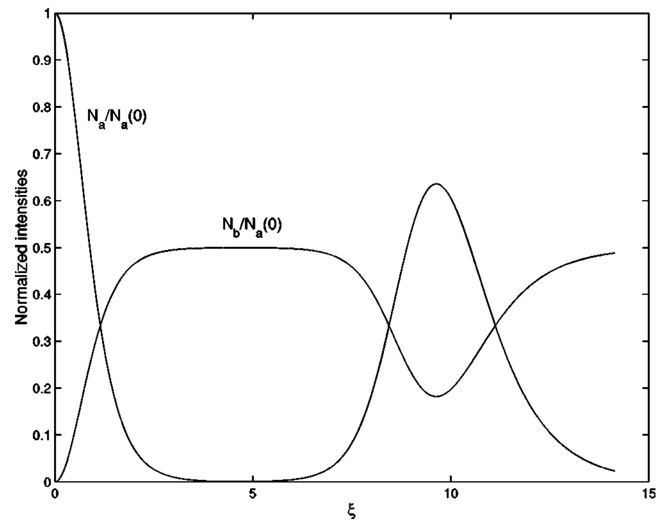

FIG. 5. The dynamics of the field intensities with increasing interaction length. In the linearized results, there is no revival in N_a, which goes monotonically to zero.

It is useful to consider the weighted sum of the three criteria,

$$\mathcal{S}_X = \tfrac{1}{2}\,[C^2_{X_b^{out}X_a^{in}} + C^2_{X_a^{out}X_a^{in}} - V(X_a^{out}|X_b^{out})], \qquad (18)$$

with a similar definition for the phase quadrature correlations. This sum will have a value of one when all three criteria are perfectly satisfied, signifying an ideal QND scheme. For our parameters, we find that $\mathcal{S}_{X\ max} \approx 0.7$, while $\mathcal{S}_{Y\ max} \approx 0.1$. This demonstrates that X_a is in fact a QND quantity, but that Y_b does not qualify. Even though Y_b satisfies the first two of the criteria better than does X_a, it falls strongly into the classical region ($\geqslant 1$) for state preparation. In the classification scheme used by Roch *et al.*, Y_b qualifies as a quantum-optical tap.

Considering Fig. 5 and Fig. 6, we can see that the interesting X-quadrature correlations are generally at their best before the point around $\xi \approx 6$, where the noise in the X_a quadrature has begun to increase and the noise in the X_b quadrature is already well above the coherent-state level. This noise increases as the process within the crystal changes from harmonic generation to down-conversion, which is at least initially a spontaneous process. It is therefore not surprising that, as shown in Fig. 7, the overall performance of the X quadratures decreases after $\xi \approx 5$.

IV. CONCLUSION

We have shown that the behavior of this system in terms of the standard QND criteria is quite different from that predicted by a linearized analysis, with nonlinear quantum effects playing an important role. In this case, not even the truncated Wigner-representation equations give correct results, once again demonstrating the dangers of unjustified

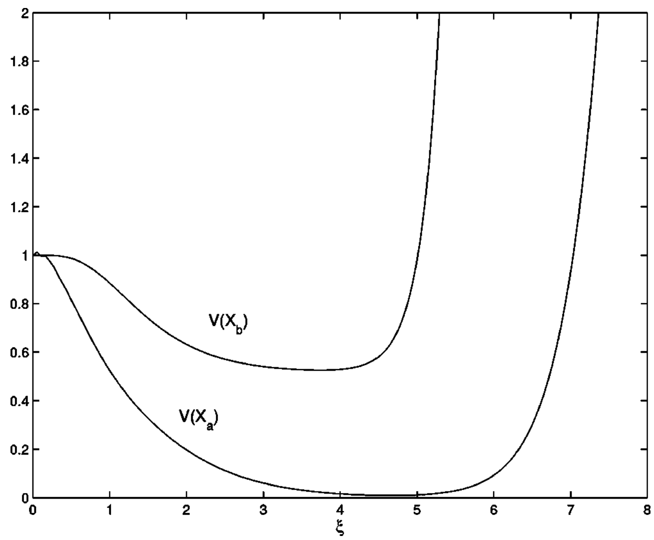

FIG. 6. The development of the amplitude quadrature variances. The linearized analysis gives asymptotic values of $V(X_a)=0$ and $V(X_b)=0.5$. The amplitude quadrature of the harmonic begins to develop excess noise over the linearized solution at $\xi\approx 4$.

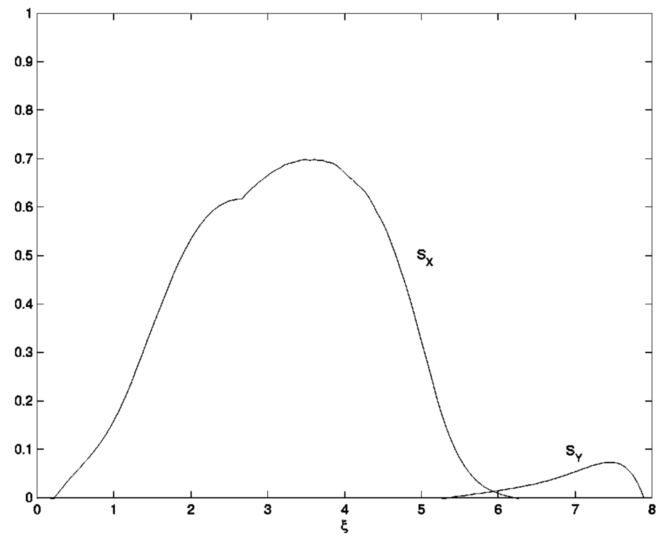

FIG. 7. The weighted sums of the three criteria for X_a and Y_b. A value of greater than one half qualifies as genuine QND.

linearization and truncation procedures.

The phase quadrature of the harmonic, which had been previously proposed as a QND quantity, fails on the grounds of state preparation. The amplitude quadrature of the fundamental, however, satisfies the state preparation criterion very well, although its behavior for measurement quality and signal degradation is inferior to the phase quadrature.

We have also shown that the performance of the device does not continue to improve with increasing interaction length, but actually worsens after a certain optimum length. This is the same region where the noise in the system has been found to increase in a previous analysis of the squeezing properties, due to the partially spontaneous nature of the down-conversion process as the fundamental revives. There is, however, a significant region in the approximate range $2\leqslant\xi\leqslant 5$ where X_a meets all the criteria, suggesting that a genuine QND measurement can be performed using this system.

The true QND region of this system should be attainable with either very high power lasers or more effective crystals. As long as the interaction region is smaller than the Rayleigh length of the light beams, our analysis in terms of plane waves should retain validity. It is also possible that in some regions there may be different quadratures displaying good correlations, which is a topic for future investigation.

ACKNOWLEDGMENTS

This research was supported by the Marsden Fund of the Royal Society of New Zealand, FAPESP (Fundação de Amparo à Pesquisa do Estado de São Paulo), and the University of Auckland Research Committee. M.K.O. wishes to thank the Physics Department of the University of Auckland for their generous hospitality.

[1] J.A. Armstrong, N. Bloembergen, J. Ducuing, and P.S. Pershan, Phys. Rev. **127**, 1918 (1962).
[2] Z.Y. Ou, Phys. Rev. A **49**, 2106 (1994).
[3] R.D. Li and P. Kumar, Phys. Rev. A **49**, 2157 (1994).
[4] R.D. Li and P. Kumar, J. Opt. Soc. Am. B **12**, 2310 (1995).
[5] M.K. Olsen, R.J. Horowicz, L.I. Plimak, N. Treps, and C.S. Fabre, Phys. Rev. A **61**, 021803(R) (2000).
[6] M.K. Olsen and R.J. Horowicz, Opt. Commun. **168**, 135 (1999).
[7] M. Dance, M.J. Collett, and D.F Walls, Phys. Rev. Lett. **66**, 1115 (1991).
[8] Ph. Grangier, J.A. Levenson, and J.-Ph. Poizat, Nature (London) **396**, 537 (1998).
[9] C.M. Caves, K.S. Thorne, R.W.P. Drever, V.D. Sandberg, and M. Zimmerman, Rev. Mod. Phys. **52**, 341 (1980).
[10] *Quantum Optics, Experimental Gravitation and Measurement Theory*, edited by P. Meystre and M.O. Scully (Plenum, New York, 1983).
[11] M.D. Levenson, R.M. Shelby, M. Reid, and D.F. Walls, Phys. Rev. Lett. **57**, 2473 (1986).
[12] V.B. Braginsky, Usp. Fiz. Nauk **156**, 93 (1988) [Sov. Phys. Usp. **31**, 836 (1988).
[13] A. LaPorta, R.E. Slusher, and B. Yurke, Phys. Rev. Lett. **62**, 28 (1989).
[14] Ph. Grangier, J.-F. Roch, and G. Roger, Phys. Rev. Lett. **66**, 1418 (1990).
[15] M.J. Holland, M.J. Collett, D.F. Walls, and M.D. Levenson, Phys. Rev. A **42**, 2995 (1990).
[16] P. Grangier, J.-M. Courty, and S. Reynaud, Opt. Commun. **89**, 99 (1992).
[17] J.F. Roch, G. Roger, P. Grangier, J.-M. Courty, and S. Reynaud, Appl. Phys. B: Photophys. Laser Chem. **55**, 291 (1992).

[18] J.-F. Roch, K. Vigneron, Ph. Grelu, A. Sinatra, J.-Ph. Poizat, and Ph. Grangier, Phys. Rev. Lett. **78**, 634 (1997).
[19] L. Mandel, Opt. Commun. **42**, 437 (1982).
[20] P.D. Drummond and C.W. Gardiner, J. Phys. A **13**, 2353 (1980).
[21] E.P. Wigner, Phys. Rev. **40**, 749 (1932).
[22] C.W. Gardiner, *Quantum Noise* (Springer-Verlag, Berlin, 1991).
[23] A. Englander, R. Lavi, M. Katz, M. Oron, D. Eger, and E. Lebiush, Opt. Lett. **22**, 1598 (1997).
[24] S. Yu and M. Weiner, J. Opt. Soc. Am. B **16**, 1300 (1999).
[25] R. Kubo, J. Phys. Soc. Jpn. **6**, 571 (1957).
[26] P.C. Martin and J. Schwinger, Phys. Rev. **115**, 1342 (1959).
[27] R. Kubo, Rep. Prog. Phys. **29**, 255 (1966).
[28] C.W. Gardiner, *Handbook of Stochastic Methods* (Springer-Verlag, Berlin, 1985).